Published in final edited form as:
Chem Res Toxicol. 2008 May ; 21(5): 1163–1170. doi:10.1021/tx800051y.

Quantitative HPLC-electrospray ionization-MS/MS analysis of the adenine-guanine cross-links of 1,2,3,4-diepoxybutane in tissues of butadiene-exposed B6C3F1 mice

Melissa Goggin, **Chris Anderson**, **Soobong Park**, **James Swenberg**[1], **Vernon Walker**[2], and **Natalia Tretyakova***

Contribution from the Cancer Center and the Department of Medicinal Chemistry, University of Minnesota, Minneapolis, MN 55455

[1] University of North Carolina at Chapel Hill, Chapel Hill, North Carolina

[2] Lovelace Respiratory Research Institute, Albuquerque, New Mexico

Abstract

1,3-Butadiene (BD) is an important industrial chemical used in the rubber and plastics manufacture, as well as an environmental pollutant present in automobile exhaust and cigarette smoke. It is classified as a known human carcinogen based on the epidemiological evidence in occupationally exposed workers and its ability to induce tumors in laboratory animals. BD is metabolically activated to several reactive species, including 1,2,3,4-diepoxybutane (DEB) which is hypothesized to be the ultimate carcinogenic species due to its bifunctional electrophilic nature and its ability to form DNA-DNA and DNA-protein cross-links. While 1,4-*bis*-(guan-7-yl)-2,3,-butanediol (*bis*-N7G-BD) is the only type of DEB-specific DNA adduct previously quantified *in vivo*, four regioisomeric guanine-adenine (G-A) cross-links have been observed *in vitro*, e.g. 1-(guan-7-yl)-4-(aden-1-yl)-2,3-butanediol (N7G-N1A-BD), 1-(guan-7-yl)-4-(aden-3-yl)-2,3,-butanediol (N7G-N3A-BD), 1-(guan-7-yl)-4-(aden-7-yl)-2,3-butanediol (N7G-N7A-BD), and 1-(guan-7-yl)-4-(aden-6-yl)-2,3-butanediol (N7G-N^6A-BD) (Park et al., *Chem. Res. Toxicol.* 2004, 17, 1638–1651). The goal of the present work was to develop an isotope dilution HPLC-ESI^+-MS/MS method for the quantitative analysis of guanine-adenine DEB cross-links in DNA extracted from BD-exposed laboratory animals. In our approach, G-A butanediol conjugates are released from the DNA backbone by thermal or mild acid hydrolysis. Following solid phase extraction, samples are subjected to capillary HPLC-positive mode electrospray ionization-tandem mass spectrometry (HPLC-ESI^+-MS/MS) analysis with $^{15}N_3$, $^{13}C_1$-labeled internal standards. The detection limit of our current method is 0.6 to 1.5 adducts per 10^8 normal nucleotides. The new method was validated by spiking G-A cross-link standards (10 fmol each) into control mouse DNA (0.1 mg), followed by sample processing and HPLC-ESI^+-MS/MS analysis. The accuracy and precision were calculated as 105 ± 17 % for N7G-N3A -BD, 102 ± 25 % for N7G-N7A-BD, and 79 ± 11 % for N7G-N^6A-BD. The regioisomeric G-A DEB adducts were formed in a concentration dependent manner in DEB-treated calf thymus DNA, with N7G-N1A-BD found in highest amounts. Under physiological conditions, N7G-N1A-BD underwent Dimroth rearrangement to N7G-N^6A-BD ($t_{1/2}$ =114 h), while hydrolytic deamination of N7G-N1A-BD to the corresponding hypoxanthine lesion was insignificant. We found that for *in vivo* samples, a greater sensitivity could be achieved if N7G-N1A-BD adducts were converted to the corresponding N7G-N^6A-BD lesions by forced Dimroth rearrangement. Liver DNA extracted from female B6C3F1 mice that underwent inhalation exposure to 625 ppm BD for 2 weeks contained 3.1

*Corresponding author: 760E CCRB, Univ. of Minnesota Cancer Center, 806 Mayo, 420 Delaware St. SE., Minneapolis, MN 55455; Tel. (612)626-3432; trety001@umn.edu.

± 0.6 N7G-N1A-BD adducts per 10^8 nucleotides (n = 5) (quantified as N7G-N^6A-BD following base-induced Dimroth rearrangement), while the amounts of N7G-N3A-BD and N7G-N7A-BD were below the detection limit of our method. None of the G-A cross-links was present in control animals. The formation of N7G-N1A-BD cross-links may contribute to the induction of AT base pair mutations following exposure to BD. Quantitative methods presented here may be used not only for studies of biological significance in animal models, but potentially to predict risk associated with human exposure to BD.

Introduction

1,3-Butadiene (BD)[1] is a large volume industrial chemical commonly used in the rubber and plastics industries, e.g., the manufacturing of styrene-butadiene rubber and tires (1). The worldwide demand for BD in 2004 was approximately 9 million metric tons (1). BD is also an environmental toxin present in automobile exhaust and cigarette smoke (20–75 μg per cigarette in mainstream smoke, 205–360 μg in sidestream smoke)(2,3). According to recent toxicological risk analyses, BD has the highest cancer risk index among all tobacco constituents (4). BD is classified as a human carcinogen based on “sufficient evidence” in humans of an increased risk for leukemias, its multi-site carcinogenicity in laboratory animals, and its pronounced genotoxic effects, including the induction of point mutations, large deletions, and chromosomal aberrations (5–10).

Chemical modification of genomic DNA by the epoxide metabolites of BD is considered an early critical event in its carcinogenic mechanisms (11). Upon metabolic activation, BD is first oxidized to 3,4-epoxy-1-butene (EB), which can be further oxidized to 1,2,3,4-diepoxybutane (DEB) or can be metabolized by epoxide hydrolase to form 1-butene-3,4-diol (12–15) (Scheme 1). DEB can also be hydrolyzed to 3,4-epoxy-1,2-butanediol (EBD) (14) and further to the corresponding tetrol. The three epoxide metabolites of BD (EB, DEB, and EBD) are reactive electrophiles capable of binding to nucleophilic sites within biomolecules to form covalent adducts (16,17).

Although DEB is a relatively minor metabolite of BD, it is considerably more genotoxic and mutagenic than its monoepoxide analogues, EB and EBD (18,19). DEB is 50x more effective in inducing sister chromatid exchanges and chromosomal aberrations in human lymphocytes than EB (20–22) and is two orders of magnitude more mutagenic than EB in TK6 lymphoblasts (23). The types of mutations induced by the two epoxides are distinct. While EB exposure results in base substitutions at GC basepairs (24), DEB induces deletions and point mutations at both AT and GC basepairs (9,25–27).

Animal studies revealed pronounced interspecies difference in sensitivity towards BD-induced cancer. In chronic inhalation experiments with B6C3F1 mice and Sprague-Dawley rats, BD was carcinogenic in both species (10,28). However, B6C3F1 mice developed tumors at BD exposure concentrations three orders of magnitude lower than those that cause cancer in Sprague-Dawley rats (10,28–30). Furthermore, the mutational spectrum found in BD-induced tumors of mice was different from that in rats (31). The increased susceptibility of mice to the carcinogenicity of BD may result from a more efficient metabolic activation of BD to DEB in this species (18,30,32). Indeed, several studies have found that target tissues of BD-exposed mice, especially lung, contain significant levels of DEB (29). DEB specific *N*,*N*-(2,3-

[1]List of Abbreviations: BD, 1,3-butadiene; bis-N7G-BD, 1,4-bis-(guan-7-yl)-2,3-butanediol; DEB, 1,2,3,4-diepoxybutane; EB, 3,4-epoxy-1-butene; EH, epoxide hydrolase; G-A, guanine-adenine; HPLC-ESI^+-MS/MS, liquid chromatography-electrospray ionization tandem mass spectrometry; N7G-N1A-BD, 1-(guan-7-yl)-4-(aden-1-yl)-2,3-butanediol; N7G-N3A-BD, 1-(guan-7-yl)-4-(aden-3-yl)-2,3,-butanediol; N7G-N7A-BD, 1-(guan-7-yl)-4-(aden-7-yl)-2,3-butanediol; N7G-N^6A-BD, 1-(guan-7-yl)-4-(aden-6-yl)-2,3-butanediol; SD, standard deviation; SRM, selected reaction monitoring; THBG, N7-(2, 3, 4-trihydroxy-1-yl)guanine

dihydroxy-1,4-butanediyl)-valine globin adducts were detected in mice treated with as little as 3 ppm BD by inhalation (15). In contrast, formation of DEB in rat tissues is negligible, providing a possible explanation for the weak tumorigenic response to BD in this species (15,29,30,33,34). Consistent with this model, all three species are equally sensitive to the genotoxic effects of DEB when it is introduced directly into isolated rat, mouse, or human lymphocytes (22,35).

The ability of DEB to induce characteristic mutations and chromosomal aberrations has been attributed to its bifunctional nature. Because of the presence of two electrophilic epoxide groups in its structure, DEB can cross-link cellular biomolecules and form exocyclic DNA lesions. We have previously identified 1,4-*bis*-(guan-7-yl)-2,3-butanediol (*bis*-N7G-BD) as the major DEB-induced DNA-DNA cross-link and quantified this lesion in liver and lung DNA of mice that had been exposed to 625 ppm BD for 5 days (36). However, guanine-guanine cross-linking by DEB cannot explain the induction of AT base pair mutations following exposure to BD and DEB (24,37,38).

In addition to guanine-guanine butanediol conjugates, DEB has been shown to form four regioisomeric adenine-guanine cross-links, e.g. 1-(guan-7-yl)-4-(aden-1-yl)-2,3-butanediol (N7G-N1A-BD), 1-(guan-7-yl)-4-(aden-3-yl)-2,3,-butanediol (N7G-N3A-BD), 1-(guan-7-yl)-4-(aden-7-yl)-2,3-butanediol (N7G-N7A-BD), and 1-(guan-7-yl)-4-(aden-6-yl)-2,3-butanediol (N7G-N^6A-BD) (Scheme 2) (39). Among these, N7G-N3A-BD and N7G-N7A-BD are thermally labile and can be spontaneously released from the DNA backbone under physiological conditions, while N7G-N1A-BD and N7G-N^6A-BD require acid hydrolysis to undergo depurination (39). In the present work, we report an HPLC-ESI^+-MS/MS method for sensitive and accurate quantitation of adenine-guanine cross-links of DEB *in vitro* and *in vivo* and its application to analyses of guanine-adenine (G-A) BD cross-links in liver DNA of BD-exposed and control female B6C3F1 mice.

Experimental Section

Note: DEB is a known carcinogen and must be handled with adequate safety precautions

Materials and Methods

Calf thymus DNA and racemic DEB were obtained from Sigma-Aldrich (St. Louis, MO). *Meso*-DEB, unlabeled N7G-N1A-BD, N7G-N3A-BD, N7G-N7A-BD, and N7G-N^6A-BD were synthesized as previously reported (39). $^{15}N_3$, $^{13}C_1$-dG was a gift from Professor Roger Jones (Rutgers University). Stock solutions of N7G-N1A-BD, N7G-N3A-BD, N7G-N7A-BD, and N7G-N^6A-BD were prepared in 0.1 M HCl and stored at −20 °C.

Synthesis of $^{15}N_3$, $^{13}C_1$-N7G-N1A-BD and $^{15}N_3$, $^{13}C_1$-N7G-N3A-BD (internal standards for mass spectrometry)

2′-Deoxyadenosine (49.7 mg), $^{15}N_3$, $^{13}C_1$-dG (8.8 mg), and glacial acetic acid (1 mL) were combined in a microcentrifuge tube and heated to 80 °C. Racemic DEB (3 μL) was added, and the mixture heated at 80 °C for 1 hour. The solution was cooled to 37 °C and 5 volumes of ether:acetone (4:1) were added. The resulting white precipitate was brought up in 0.1 M HCl and hydrolyzed at 80 °C for 1 hour. The products were purified by HPLC using a Luna C18 (4.6 × 150 mm) column. G-A cross-links were isolated using a gradient from 0 to 6% acetonitrile (B) in 20 mM ammonium acetate, pH 4.9 (A) in 6 minutes, and further to 10 % B in14 minutes. Under these conditions, $^{15}N_3$, $^{13}C_1$- N7G-N1A-BD eluted at 9.8 minutes and $^{15}N_3$, $^{13}C_1$- N7G-N3A-BD eluted at 10.5 minutes. Internal standard stock solution concentrations were determined by comparing LC-MS/MS peak areas with peak areas of analyte of known concentration.

Animals and treatment

B6C3F1 mice were purchased from Charles River Laboratories (Wilmington, MA) and were acclimated for about 10 days before initiation of chemical exposures. Animals were randomly separated into air-control and exposure groups by weight and were housed individually in hanging wire stainless steel cages according to NIH guidelines (NIH Publication 86-23, 1985). All procedures involving the use of animals were approved by the Institutional Animal Care and Use Committee.

Experimental animals were exposed using multi-tiered whole-body exposure chambers (H-2000, Lab Products, Aberdeen, MD). Rodents in one chamber received filtered air only as a control group, and rodents in the other chamber received nominal 625 ppm BD for 2 weeks (6 h/day, 5 days/week). Animals were housed within exposure chambers throughout the experiment, and had free access to food and water except for removal of food during the 6-h exposure periods. Within 2 hours after cessation of the final day of exposure, animals were euthanized *via* cardiac puncture, and tissues were harvested and snap-frozen for storage at −80° C.

DNA isolation

Liver tissue (0.1–0.5 g) was homogenized in Tris-EDTA buffer (10 mL), and DNA was extracted by previously reported methods (36). DNA purity and amounts were determined by UV spectrophotometry. Typical A_{260}/A_{280} ratios were between 1.7 and 1.9, ensuring minimal protein contamination.

DNA hydrolysis and sample preparation

DNA samples (100 μg, dissolved in 300 μl water) were spiked with $^{15}N_3$, $^{13}C_1$-N7G-N3A-BD (300 fmol) and subjected to neutral thermal hydrolysis (70 °C for 1 hour) to release thermally labile adducts (N7G-N7A-BD and N7G-N3A-BD). The partially depurinated DNA was removed by Centricon YM-10 filtration (Millipore Corp., Billerica, MA), while the filtrates containing N7G-N7A-BD, N7G-N3A-BD, and $^{15}N_3$, $^{13}C_1$- N7G-N3A-BD were stored at −20 °C until further analysis. Partially depurinated DNA was recovered by reversing the filters and washing with water into new collection tubes according to manufacturer's instructions. The partially depurinated DNA was spiked with $^{15}N_3$, $^{13}C_1$-N7G-N1A-BD internal standard (300 fmol), and subjected to mild acid hydrolysis (0.1 M HCl at 70 °C for 30 min) to release all purine bases including N7G-N1A-BD and N7G-N^6A-BD. Following Centricon YM-10 filtration to remove the DNA backbone, pH was adjusted to 12 with 0.2 M NaOH, and the solutions were incubated at 70 °C overnight to induce Dimroth rearrangement of N7G-N1A-BD adducts to the corresponding N7G-N^6A-BD species. The resulting samples were neutralized with HCl prior to solid phase extraction.

Solid phase extraction

DNA hydrolysates containing G-A DEB adducts were purified by solid phase extraction. Sep Pak C18 cartridges (100 mg, 1 ml, Waters Corp., Millford, MA) were equilibrated with methanol (1 mL) and water (3 × 1 mL) prior to loading samples in 0.05 M $NaHCO_3$ (1 mL). The hydrolysates were washed with water (2 × 1 mL), and eluted with 50 % methanol (1 mL). The eluates were dried under vacuum and resuspended in 0.05% acetic acid (25 μL) for HPLC-ESI^+-MS/MS analysis (injection volume, 8 μL).

HPLC-ESI^+-MS/MS

An Agilent 1100 capillary HPLC system (Wilmington, DE) interfaced to a Finnigan TSQ Quantum triple quadrupole mass spectrometer was used in all analyses. Chromatographic separation was achieved with a Zorbax SB-C18 column (150 × 0.5 mm, 5 μm) eluted at a flow

rate of 15 μL/min. The solvent system consisted of 0.05% acetic acid (A) and methanol (B). A linear gradient from 3 to 9% B in 5 minutes and further to 24% B in 3 minutes was employed.

The regioisomeric G-A cross-links of DEB were quantified by isotope dilution with $^{15}N_3$, $^{13}C^1$-labeled internal standards. $^{15}N_3$, $^{13}C_1$-N7G-N3A-BD was used as an internal standard for quantitation of both N7G-N3A-BD and N7G-N7A-BD as they are both released from DNA by neutral thermal hydrolysis. $^{15}N_3$, $^{13}C^1$-N7G-N1A-BD was used as an internal standard for quantitation of both N7G-N1A-BD and N7G-N^{6}A-BD as these cross-links are analyzed in acid hydrolysates.

Quantitative analyses of DEB-induced G-A cross-links were performed using HPLC-ESI$^+$-MS/MS peak areas corresponding to the loss of guanine (*m/z* 373.1 $[M + H]^+ \rightarrow$ *m/z* 222.1 $[M + H - Gua]^+$) or the loss of adenine and water (*m/z* 373.1 $[M+H]^+ \rightarrow$ 220.0 $[M+H\text{-}Ade\text{-}H_2O]^+$) from protonated molecules of the adducts (M = 372). $^{15}N_3$, $^{13}C_1$-N7G-Ade-BD internal standards (M = 376) were analyzed analogously by following the transitions *m/z* 377.1 $[M + H]^+ \rightarrow$ *m/z* 222.0 $[M+H\text{-}^{15}N_3, ^{13}C_1\text{-}Gua]$ + and *m/z* 377.1 $[M+H]^+ \rightarrow$ *m/z* 224.0 $[M+H\text{-}Ade\text{-}H_2O]^+$. Calibration curves were constructed by analyzing solutions containing known amounts of N7G-Ade-BD standards and $^{15}N_3$, $^{13}C_1$-GA internal standards.

HPLC-ESI$^+$-MS/MS method validation

A method calibration curve was constructed by spiking control mouse liver DNA (100 μg) with known amounts of N7G-Ade-BD cross-links (0 to 500 fmol) and isotopically-labeled internal standard (500 fmol). Validation samples were processed and analyzed by HPLC-ESI$^+$-MS/MS in the same manner as actual samples.

Calf thymus DNA treatment with DEB and sample processing

Calf thymus DNA (500 μg, in triplicate) was dissolved in 500 μl of 10 mM Tris-HCl buffer, pH 7.2, and incubated with varying concentrations of racemic or *meso* DEB at 37 °C for 24 hours. The reaction mixtures were extracted with diethyl ether (2 × 400 μL) to remove unreacted DEB. Internal standard, $^{15}N_3$, $^{13}C_1$-N7G-N3A-BD (25 pmol) was added, and samples were subjected to neutral thermal hydrolysis (70 °C for 1 hour) to release N7G-N7A-BD and N7G-N3A-BD adducts. Partially depurinated DNA was removed by Centricon YM-30 ultrafiltration, and the filtrates containing N7G-N7A-BD and N7G-N3A-BD were dried under vacuum and reconstituted in 100 μL of water prior to HPLC- ESI$^+$-MS/MS analysis. The DNA was recovered from the filter, spiked with $^{15}N_3$, $^{13}C_1$-N7G-N1A-BD internal standard (25 pmol), and subjected to mild acid hydrolysis to release N7G-N1A-BD and N7G-N^{6}A-BD (0.1 M HCl at 70 °C for 30 minutes). Samples were filtered through Centricon YM-30 filters, concentrated to 100 μL under vacuum, and analyzed by HPLC- ESI$^+$-MS/MS.

Stability study of N7G-N1A-BD

Authentic N7G-N1A-BD (10 pmol) dissolved in 10 mM Tris-HCl (pH 7.2, 250 μl) and incubated at 37 °C. Aliquots (25 μl) were removed at various time points (2–72 hours) and immediately frozen. Aliquots were analyzed by capillary HPLC-ESI$^+$ MS/MS as described above by using the transitions *m/z* 373 → 222 for N7G-N1A-BD, N7G-N^{6}A-BD and *m/z* 374 → 223 for N7G-N1HX. Peak areas were normalized to N7G-N1A-BD and plotted as a function of time.

Results

Development of quantitative HPLC-ESI$^+$-MS/MS method for G-A DEB adducts

To enable sensitive and specific detection of guanine-adenine cross-links of DEB (Scheme 2) in biological samples, isotope dilution HPLC-ESI$^+$-MS/MS methodology was developed. In

our approach, G-A cross-links are quantified as nucleobase conjugates following their release from the DNA backbone by neutral thermal hydrolysis (N7G-N3A-BD, N7G-N7A-BD) or acid hydrolysis (N7G-N1A-BD and N7G-N^6A-BD). Early in the analysis, DNA is spiked with $^{15}N_3$, $^{13}C_1$-N7G-N3A-BD internal standard, followed by neutral thermal hydrolysis to release N7G- N7A-BD and N7G-N3A-BD adducts (Scheme 3). Centricon ultrafiltration is used to remove the partially depurinated DNA, which is then spiked with $^{15}N_3$, $^{13}C_1$-N7G-N1A-BD internal standard and subjected to mild acid hydrolysis to release N7G-N1A-BD and N7G-N^6A-BD. G-A BD lesions and their internal standards are purified by solid phase extraction on SepPak C18 cartridges. Quantitative analysis of the G-A BD regioisomers is performed by capillary HPLC-ESI^+-MS/MS. The mass spectrometer is operated in the selected reaction monitoring mode by following the transitions corresponding to the neutral loss of adenine base and water or guanine base from the protonated molecules of the adducts, *m/z* 373.1 $[M + H]^+ \rightarrow$ *m/z* 220.1 [M + H – Ade – H_2O]+ and *m/z* 373.1 $[M + H]^+ \rightarrow$ *m/z* 222.1 [M + H – Gua]$^+$. $^{15}N_3$, $^{13}C_1$-labeled internal standards are analyzed analogously using the transitions *m/z* 377.1 → *m/z* 224.1, *m/z* 222.1. $^{15}N_3$, $^{13}C_1$-N7G-N3A-BD internal standard was used to quantify the depurinating G-A cross-links (N7G-N7A-BD and N7G-N3A-BD) (Figure 1A), while $^{15}N_3$, $^{13}C_1$-N7G-N1A-BD internal standard was used to quantify the thermally stable G-A adducts (N7G-N1A-BD and N7G-N^6A-BD) (Figure 1B). Based on calibration curves, N7G-N7A-BD had approximately 2-fold greater HPLC-ESI^+-MS/MS response as compared with N7G-N3A-BD (Figure 2A), while N7G-N1A-BD had a 3-fold higher HPLC-ESI^+-MS/MS response than N7G-N^6A-BD (Figure 2B).

Concentration dependence curves in DEB-treated DNA

To quantify the formation of regioisomeric G-A DEB cross-links *in vitro*, calf thymus DNA was treated with racemic or *meso* DEB (0–1000 μM), followed by HPLC-ESI^+-MS/MS analysis of the resulting G-A cross-links with the newly developed methods. Adduct amounts increased linearly with increased DEB concentration (Figure 3). We found that the major G-A BD cross-link formed was N7G-N1A-BD, followed by N7G-N7A-BD, N7G-N3A-BD, and N7G-N^6A-BD. N7G-N^6A-BD amounts were below the detection limit in samples treated with low DEB concentrations (< 500 μM). Consistent with our previous findings (39), N7G-N1A-BD was the most abundant N7G-Ade-BD cross-link formed *in vitro*. No stereospecific differences in adduct amounts were observed in DNA treated with racemic or *meso* DEB (Supplement S-1).

Method validation

Method calibration curves were obtained by spiking control mouse liver DNA with known amounts of G-A BD cross-links and the corresponding $^{15}N_3$, $^{13}C_1$-internal standards, followed by HPLC-ESI+-MS/MS analysis by the same methods. Forced Dimroth rearrangement was employed to convert N7G-N1A-BD to N7G-N^6A-BD because of the interfering signal originating from liver DNA hydrolysates that co-eluted with N7G-N1A-BD. A good correlation was observed between the expected and measured levels of N7G-Ade-BD spiked in mouse liver DNA (Figure 4). Accuracy and precision were obtained for the three cross-links at 10 fmol per 100 μg mouse liver DNA. For 5 replicate samples analyzed on 3 separate days, the calculated amounts of N7G-N3A-BD, N7G-N7A-BD, and N7G-N^6A-BD were 105 ± 17%, 102 ± 25%, and 79 ± 11% of the theoretical value, respectively (Table 1). The limits of quantitation (S/N > 10) for N7G-N3A-BD, N7G-N7A-BD, and N7G-N^6A-BD spiked into 100 μg of mouse DNA were 1.5–3 adducts per 10^8 nucleotides, while the limits of detection (S/N > 3) 0.6–1.5 adducts per 10^8 nucleotides. The limits of quantitation for pure standards were 3–5 fmol (S/N 25–34), with the limits of detection of 1 fmol.

In vivo analysis of N7G-Ade-BD

DNA extracted from liver tissue of female B6C3F1 mice exposed to 625 ppm BD for 10 days by inhalation and the corresponding air-only controls was analyzed using the new quantitative HPLC-MS/MS method. We found that DNA isolated from liver of BD-exposed mouse contained 3.1 ± 0.58 N7G-N1A-BD per 10^8 nucleotides (N = 5, quantified as N7G-N^{6}A-BD following forced Dimroth rearrangement), while control DNA did not contain any N7G-N1A-BD lesions (Table 2). The amounts of N7G-N3A-BD and N7G-N7A-BD in the same animals were below the limits of detection of our current methods (1.5 adducts per 10^8 nucleotides). Representative HPLC-ESI$^+$-MS/MS chromatograms of a control and BD-exposed mouse DNA are shown in Figure 5.

Discussion

BD is an important industrial chemical classified as a probable human carcinogen based on laboratory animal studies and human epidemiology data. However, human risk assessment from exposure to BD is complicated because of the documented interspecies differences in metabolism and carcinogenic response (19,40). Because of its central role in BD-mediated genotoxicity, DEB-specific biomarkers of BD exposure are needed to identify adducts responsible for BD-associated mutagenesis, and to determine which animal model will be most suitable in evaluating human risks associated with BD exposure.

DEB causes a large number of A to T transversion mutations (24,38), yet previous studies have failed to identify DEB-DNA adducts responsible for these genetic changes. Polymerase bypass of synthetic DNA templates containing N^6-(2,3,4-trihydroxybut-1-yl)-adenine monoadducts of *(R,R)* and *(S,S)* DEB is mostly error-free, leading to low levels of A → G and A → C base substitutions (< 0.3%) (41). N1-(2,3,4-trihydroxybut-1-yl)-dI lesions originating by deamination of the corresponding N1-dA adducts can induce high levels of A → G transitions (42), but these lesions have not been detected *in vivo*. None of the DEB monoadducts tested induced A → T transversions, limiting our understanding of the structural origins of BD-mediated mutagenesis.

Earlier *in vivo* analyses of DEB-DNA adducts have been limited to DEB-induced trihydroxybutyl monoadducts, e.g. N7-(2,3,4-trihydroxybut-1-yl) guanine (N7-THBG) and N^6-(2,3,4-trihydroxybut-1-yl)-Ade (43). These monoadducts are not DEB-specific because they can be formed by another, more abundant BD metabolite, EBD (Scheme 1). Recently, our laboratory has developed sensitive and specific methods for the quantification of guanine-guanine cross-links of DEB (*bis*-N7G-BD). We found that mouse liver DNA from animals exposed to 625 ppm BD for 1 week contained 8.9 *bis*-N7G-BD adducts per 10^7 normal nucleotides. Unlike trihydroxybutyl monoadducts, *bis*-N7G-BD lesions can only be formed by DEB and represent a specific biomarker of exposure to DEB.

In the present work, we developed and validated a sensitive and specific isotope dilution HPLC-ESI$^+$-MS/MS method for the quantitative analysis of G-A cross-links of DEB. Using our new method, N7G-N^{6}A-BD was detected in DNA extracted from liver tissue of mice exposed to BD (625 ppm for 10 days). As expected from *in vitro* studies, levels of N7G-N^{6}A-BD (3.08 ± 0.58/10^8 nucleotides) were an order of magnitude lower than the amounts of *bis*-N7G-BD adducts in the same animals (3.9 adducts/10^7 nucleotides).[2] Neither N7G-N3A-BD nor N7G-N7A-BD were detected *in vivo*, which may be explained by their rapid spontaneous depurination at physiological conditions ($t_{1/2}$ = 35 and 17 h, respectively (39)).

[2]Goggin and Tretyakova, manuscript in preparation

Although in the present study, a sum of N7G-N1A-BD and N7G-N^6A-BD adduct was quantified following forced Dimroth rearrangement of N7G-N1A-BD to N7G-N^6A-BD (Scheme 4), we hypothesize that N7G-N1A-BD is the dominant G-A cross-link *in vivo* based on the following evidence. N7G-N1A-BD is by far the most abundant G-A conjugate following *in vitro* treatment of double stranded DNA with DEB (Figure 3) and is very stable at physiological conditions, undergoing only minimal rearrangement to N7G-N^6A-BD (< 16 % at 72 h) (Figure 6). Hydrolytic deamination of N7G-N1A-BD to the corresponding hypoxanthine-guanine cross-link (N1HX-N7G-BD) (44) is even slower (1.4 % following 72 h incubation) and may not be relevant in cells.

The biological significance of the formation of G-A DEB conjugates in BD-exposed animals remains to be established. Although their concentrations are only 1/10 of the amounts of the dominant G-G DNA cross-links of DEB (*bis*-N7G-BD), N7G-N1A-BD and N7G-N^6A-BD conjugates are more hydrolytically stable and may accumulate in target tissues over time (45). For example, Koivisto et al. observed higher levels of N7-THBG lesions than N^6-THBA *in vivo* immediately following BD exposure, however, no N7-THBG was detected 21 days post exposure, while the concentrations of N^6-THBA remained the same (46). Spontaneous hydrolysis of the N7-substituted guanine moiety within N7G-N1A-BD and N7G-N^6A-BD under physiological conditions would lead to the formation of a bulky adduct opposite an abasic site (Scheme 5). Repair of such a lesion is likely to be hindered or promutagenic because of the presence of DNA damage in both strands of DNA.

The quantitative HPLC-ESI^+-MS/MS methods presented in this work will allow future analyses of BD dose-response relationships, repair, and accumulation of DEB-specific G-A cross-links *in vivo*. Interspecies differences in metabolism of BD have been observed in studies with human, rat and mouse microsomes (47). Mice metabolize BD to DEB at faster rates than rats and humans do (48), which suggests that greater amounts of DEB-specific lesions such as N7G-N^6A-BD and *bis*-N7G-BD may be formed in the mouse. Furthermore, there may be interspecies differences in repair of N7G-N1A-BD cross-links. The availability of DEB-specific biomarkers of DNA adducts will facilitate future studies of such interspecies variations in BD induced cancer, which is required for setting industrial BD exposure limits. Studies are currently in progress to investigate the dose-dependent formation and repair of N7G-N1A-BD in BD-exposed mice and rats.

Supplementary Material

Refer to Web version on PubMed Central for supplementary material.

Acknowledgments

We thank Brock Matter (University of Minnesota Cancer Center) for help with mass spectrometry, Bimi Bisht (University of Minnesota Cancer Center) for help with N7G-N1A-BD stability experiments, and Bob Carlson (University of Minnesota Cancer Center) for help with figures for this manuscript. This work was supported by grants from the National Cancer Institute (C.A. 100670, N.T.), ES012689 (J.S.), P30-ES10126 (J.S.), Health Effects Institute (Agreement 05–12) (V.W., N.T.), and the American Chemistry Council (OLF-163.0, N.T.).

Reference List

1. White WC. Butadiene production process overview. Chem Biol Interact 2007;166:10–14. [PubMed: 17324391]
2. Pelz N, Dempster NM, Shore PR. Analysis of low molecular weight hydrocarbons including 1,3-butadiene in engine exhaust gases using an aluminum oxide porous-layer open-tubular fused-silica column. J Chromatogr Sci 1990;28:230–235. [PubMed: 1704381]

3. Hecht SS. Tobacco smoke carcinogens and lung cancer. J Natl Cancer Inst 1999;91:1194–1210. [PubMed: 10413421]
4. Fowles J, Dybing E. Application of toxicological risk assessment principles to the chemical constituents of cigarette smoke. Tob Control 2003;12:424–430. [PubMed: 14660781]
5. Stayner LT, Dankovic DA, Smith RJ, Gilbert SJ, Bailer AJ. Human cancer risk and exposure to 1,3-butadiene--a tale of mice and men. Scand J Work Environ Health 2000;26:322–330. [PubMed: 10994798]
6. Melnick RL, Huff J, Chou BJ, Miller RA. Carcinogenicity of 1,3-butadiene in C57BL/6 x C3H F1 mice at low exposure concentrations. Cancer Res 1990;50:6592–6599. [PubMed: 2208121]
7. Melnick RL, Shackelford CC, Huff J. Carcinogenicity of 1,3-butadiene. Environ Health Perspect 1993;100:227–236. [PubMed: 8354171]
8. Ward JB Jr, Ammenheuser MM, Bechtold WE, Whorton EB Jr, Legator MS. *hprt* mutant lymphocyte frequencies in workers at a 1,3-butadiene production plant. Environ Health Perspect 1994;102(Suppl 9):79–85. [PubMed: 7698091]
9. Cochrane JE, Skopek TR. Mutagenicity of butadiene and its epoxide metabolites: II. Mutational spectra of butadiene, 1,2-epoxybutene and diepoxybutane at the *hprt* locus in splenic T cells from exposed B6C3F1 mice. Carcinogenesis 1994;15:719–723. [PubMed: 8149486]
10. Melnick, RL.; Huff, JE. 1,3-Butadiene induces cancer in experimental animals at all concentrations from 6.25 to 8000 parts per million. IARC Sci. Publ; 1993. p. 309-322.
11. de Meester C. Genotoxic properties of 1,3-butadiene. Mutat Res 1988;195:273–281. [PubMed: 3283543]
12. Malvoisin E, Roberfroid M. Hepatic microsomal metabolism of 1,3-butadiene. Xenobiotica 1982;12:137–144. [PubMed: 7090423]
13. Himmelstein MW, Turner MJ, Asgharian B, Bond JA. Metabolism of 1,3-butadiene: inhalation pharmacokinetics and tissue dosimetry of butadiene epoxides in rats and mice. Toxicology 1996;113:306–309. [PubMed: 8901914]
14. Krause RJ, Elfarra AA. Oxidation of butadiene monoxide to *meso*- and (+/−)-diepoxybutane by cDNA-expressed human cytochrome P450s and by mouse, rat, and human liver microsomes: evidence for preferential hydration of *meso*-diepoxybutane in rat and human liver microsomes. Arch Biochem Biophys 1997;337:176–184. [PubMed: 9016811]
15. Filser JG, Hutzler C, Meischner V, Veereshwarayya V, Csanady GA. Metabolism of 1,3-butadiene to toxicologically relevant metabolites in single-exposed mice and rats. Chem Biol Interact 2007;166:93–103. [PubMed: 16616907]
16. Tretyakova NY, Lin YP, Upton PB, Sangaiah R, Swenberg JA. Macromolecular adducts of butadiene. Toxicology 1996;113:70–76. [PubMed: 8901884]
17. Swenberg JA, Koc H, Upton PB, Georguieva N, Ranasinghe A, Walker VE, Henderson R. Using DNA and hemoglobin adducts to improve the risk assessment of butadiene. Chem Biol Interact 2001;135–136:387–403.
18. Henderson RF, Barr EB, Belinsky SA, Benson JM, Hahn FF, Menache MG. 1,3-butadiene: cancer, mutations, and adducts. Part I: Carcinogenicity of 1,2,3,4-diepoxybutane. Res Rep Health Eff Inst 2000:11–43. [PubMed: 10925838]
19. Swenberg JA, Boysen G, Georgieva N, Bird MG, Lewis RJ. Future directions in butadiene risk assessment and the role of cross-species internal dosimetry. Chem Biol Interact 2007;166:78–83. [PubMed: 17343837]
20. Sasiadek M, Norppa H, Sorsa M. 1,3-Butadiene and its epoxides induce sister-chromatid exchanges in human lymphocytes *in vitro*. Mutat Res 1991;261:117–121. [PubMed: 1922154]
21. Kligerman AD, DeMarini DM, Doerr CL, Hanley NM, Milholland VS, Tennant AH. Comparison of cytogenetic effects of 3,4-epoxy-1-butene and 1,2:3, 4- diepoxybutane in mouse, rat and human lymphocytes following in vitro G0 exposures. Mutat Res 1999;439:13–23. [PubMed: 10029668]
22. Kligerman AD, Hu Y. Some insights into the mode of action of butadiene by examining the genotoxicity of its metabolites. Chem Biol Interact. 2006 Epub ahead of print 4/18/2006.
23. Cochrane JE, Skopek TR. Mutagenicity of butadiene and its epoxide metabolites: I. Mutagenic potential of 1,2-epoxybutene, 1,2,3,4-diepoxybutane and 3,4-epoxy-1,2- butanediol in cultured human lymphoblasts. Carcinogenesis 1994;15:713–717. [PubMed: 8149485]

24. Recio L, Steen AM, Pluta LJ, Meyer KG, Saranko CJ. Mutational spectrum of 1,3-butadiene and metabolites 1,2-epoxybutene and 1,2,3,4-diepoxybutane to assess mutagenic mechanisms. Chem Biol Interact 2001;135–136:325–341.
25. Steen AM, Meyer KG, Recio L. Characterization of *hprt* mutations following 1,2-epoxy-3-butene exposure of human TK6 cells. Mutagenesis 1997;12:359–364. [PubMed: 9379915]
26. Steen AM, Meyer KG, Recio L. Analysis of *hprt* mutations occurring in human TK6 lymphoblastoid cells following exposure to 1,2,3,4-diepoxybutane. Mutagenesis 1997;12:61–67. [PubMed: 9106245]
27. Meng Q, Singh N, Heflich RH, Bauer MJ, Walker VE. Comparison of the mutations at Hprt exon 3 of T-lymphocytes from B6C3F1 mice and F344 rats exposed by inhalation to 1,3-butadiene or the racemic mixture of 1,2:3,4-diepoxybutane. Mutat Res 2000;464:169–184. [PubMed: 10648904]
28. Owen PE, Glaister JR, Gaunt IF, Pullinger DH. Inhalation toxicity studies with 1,3-butadiene. 3 Two year toxicity/carcinogenicity study in rats. Am Ind Hyg Assoc J 1987;48:407–413. [PubMed: 3591659]
29. Thornton-Manning JR, Dahl AR, Bechtold WE, Griffith WC Jr, Henderson RF. Disposition of butadiene monoepoxide and butadiene diepoxide in various tissues of rats and mice following a low-level inhalation exposure to 1,3-butadiene. Carcinogenesis 1995;16:1723–1731. [PubMed: 7634396]
30. Henderson RF, Thornton-Manning JR, Bechtold WE, Dahl AR. Metabolism of 1,3-butadiene: species differences. Toxicology 1996;113:17–22. [PubMed: 8901878]
31. Meng Q, Singh N, Heflich RH, Bauer MJ, Walker VE. Comparison of the mutations at Hprt exon 3 of T-lymphocytes from B6C3F1 mice and F344 rats exposed by inhalation to 1,3-butadiene or the racemic mixture of 1,2:3,4-diepoxybutane. Mutat Res 2000;464:169–184. [PubMed: 10648904]
32. Jelitto B, Vangala RR, Laib RJ. Species differences in DNA damage by butadiene: role of diepoxybutane. Arch Toxicol Suppl 1989;13:246–249. [PubMed: 2774939]
33. Boysen G, Georgieva NI, Upton PB, Jayaraj K, Li Y, Walker VE, Swenberg JA. Analysis of diepoxide-specific cyclic N-terminal globin adducts in mice and rats after inhalation exposure to 1,3-butadiene. Cancer Res 2004;64:8517–8520. [PubMed: 15574756]
34. Filser JG, Hutzler C, Meischner V, Veereshwarayya V, Csanady GA. Metabolism of 1,3-butadiene to toxicologically relevant metabolites in single-exposed mice and rats. Chem Biol Interact in press. 2006
35. Kligerman AD, DeMarini DM, Doerr CL, Hanley NM, Milholland VS, Tennant AH. Comparison of cytogenetic effects of 3,4-epoxy-1-butene and 1,2:3, 4- diepoxybutane in mouse, rat and human lymphocytes following in vitro G0 exposures. Mutat Res 1999;439:13–23. [PubMed: 10029668]
36. Goggin M, Loeber R, Park S, Walker V, Wickliffe J, Tretyakova N. HPLC-ESI^{+}-MS/MS analysis of *N7*-guanine-*N7*-guanine DNA cross-links in tissues of mice exposed to 1,3-butadiene. Chem Res Toxicol 2007;20:839–847. [PubMed: 17455958]
37. Meng Q, Singh N, Heflich RH, Bauer MJ, Walker VE. Comparison of the mutations at Hprt exon 3 of T-lymphocytes from B6C3F1 mice and F344 rats exposed by inhalation to 1,3-butadiene or the racemic mixture of 1,2:3,4-diepoxybutane. Mutat Res 2000;464:169–184. [PubMed: 10648904]
38. Kim MY, Park S, Tretyakova NY, Wogan GN. Mutagenesis of 1,2,3,4-diepoxybutane in the *supF* gene: role of stereochemistry. Chem Res Toxicol. 2007 In Press.
39. Park S, Hodge J, Anderson C, Tretyakova NY. Guanine-adenine cross-linking by 1,2,3,4-diepoxybutane: potential basis for biological activity. Chem Res Toxicol 2004;17:1638–1651. [PubMed: 15606140]
40. Kligerman AD, Hu Y. Some insights into the mode of action of butadiene by examining the genotoxicity of its metabolites. Chem Biol Interact 2007;166:132–139. [PubMed: 16698003]
41. Carmical JR, Kowalczyk A, Zou Y, Van Houten B, Nechev LV, Harris CM, Harris TM, Lloyd RS. Butadiene-induced intrastrand DNA cross-links: a possible role in deletion mutagenesis. J Biol Chem 2000;275:19482–19489. [PubMed: 10766753]
42. Kanuri M, Nechev LV, Tamura PJ, Harris CM, Harris TM, Lloyd RS. Mutagenic spectrum of butadiene-derived N1-deoxyinosine adducts and N^6,N^6-deoxyadenosine intrastrand cross-links in Mammalian cells. Chem Res Toxicol 2002;15:1572–1580. [PubMed: 12482239]

43. Tretyakova NY, Chiang SY, Walker VE, Swenberg JA. Quantitative analysis of 1,3-butadiene-induced DNA adducts *in vivo* and *in vitro* using liquid chromatography electrospray ionization tandem mass spectrometry. J Mass Spectrom 1998;33:363–376. [PubMed: 9597770]
44. Tretyakova NY, Livshits A, Park S, Bisht B, Goggin M. Structural elucidation of a novel DNA-DNA cross-link of 1,2,3,4-diepoxybutane. Chem Res Toxicol 2007;20:284–289. [PubMed: 17305410]
45. Singer, B.; Grunberger, D. Molecular Biology of Mutagens and Carcinogens. Plenum Press; New York and London: 1983.
46. Koivisto P, Kostiainen R, Kilpelainen I, Steinby K, Peltonen K. Preparation, characterization and ^{32}P-postlabeling of butadiene monoepoxide N^6-adenine adducts. Carcinogenesis 1995;16:2999–3007. [PubMed: 8603476]
47. Nieusma JL, Claffey DJ, Maniglier-Poulet C, Imiolczyk T, Ross D, Ruth JA. Stereochemical aspects of 1,3-butadiene metabolism and toxicity in rat and mouse liver microsomes and freshly isolated rat hepatocytes. Chem Res Toxicol 1997;10:450–456. [PubMed: 9114983]
48. Henderson RF. Species differences in the metabolism of olefins: implications for risk assessment. Chem Biol Interact 2001;135–136:53–64.

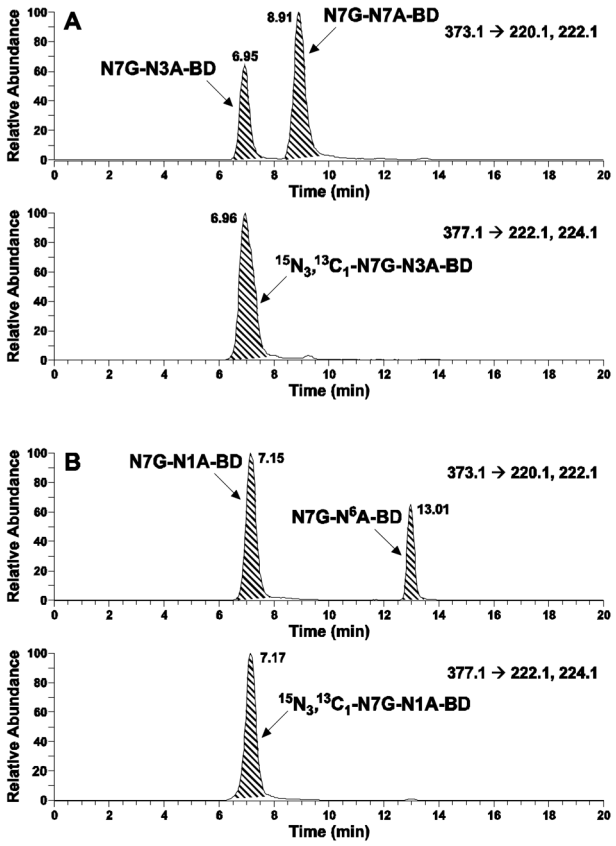

Figure 1.

Extracted ion chromarograms for HPLC-ESI$^+$-MS/MS analysis of hydrolytically-labile G-A DEB cross-links, 1-(guan-7-yl)-4-(aden-3-yl)-2,3,-butanediol (N7G-N3A-BD) and 1-(guan-7-yl)-4-(aden-7-yl)-2,3-butanediol (N7G-N7A-BD), spiked with their internal standard, $^{15}N_3$, $^{13}C_1$-N7G-N3A-BD (A) and hydrolytically-stable G-A DEB cross-links, 1-(guan-7-yl)-4- (aden-1-yl)-2,3-butanediol (N7G-N1A-BD) and 1-(guan-7-yl)-4-(aden-6-yl)-2,3-butanediol (N7G-N^{6}A-BD), spiked with their internal standard, $^{15}N_3$, $^{13}C_1$-N7G-N1A-BD (B).

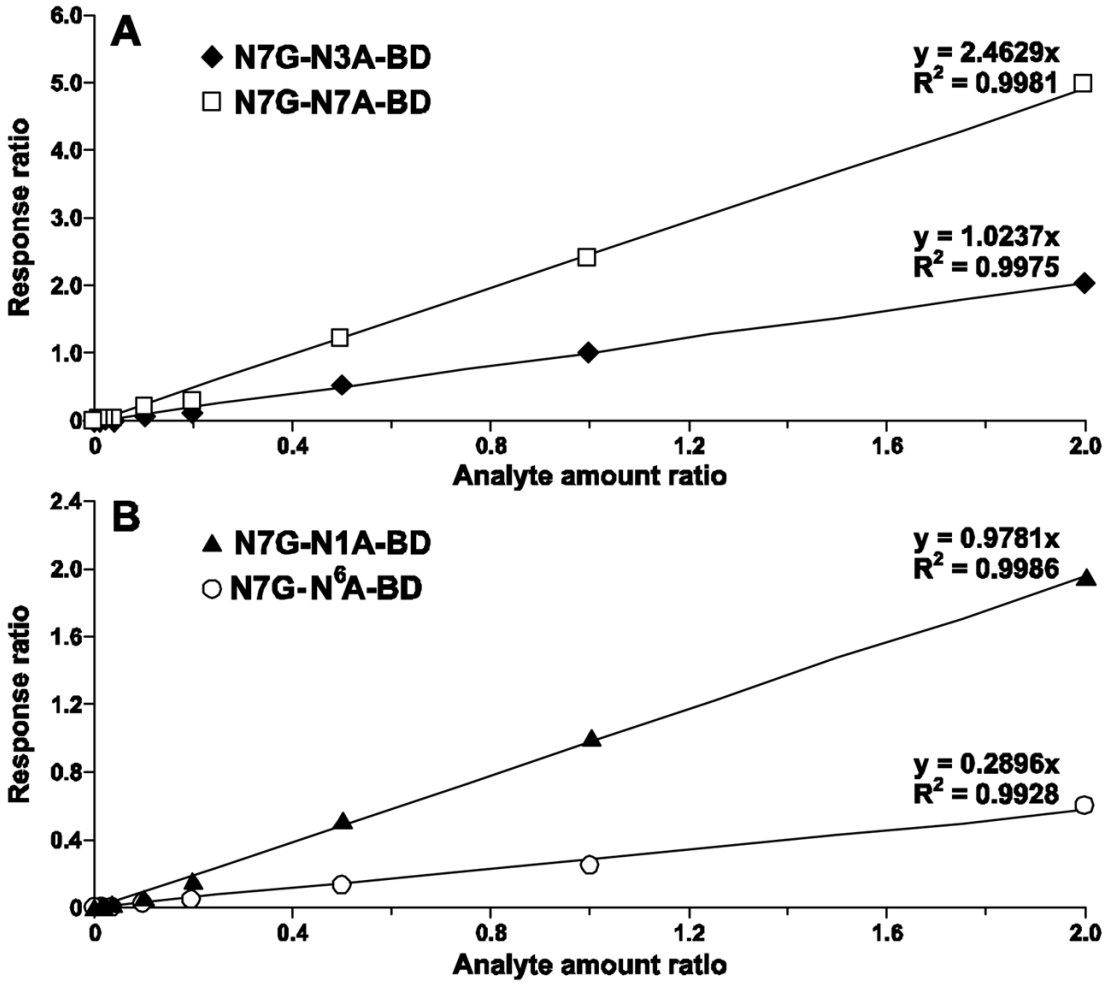

Figure 2.

Calibration curves for HPLC-ESI$^+$-MS/MS analysis of pure standards of N7G-N3A-BD and N7G-N7A-BD (A) and N7G-N1A-BD and N7G-N6A-BD (B) by isotope dilution with [$^{15}N_3$, $^{13}C_1$] N7G-N3A-BD and [$^{15}N_3$, $^{13}C_1$] N7G-N1A-BD, respectively.

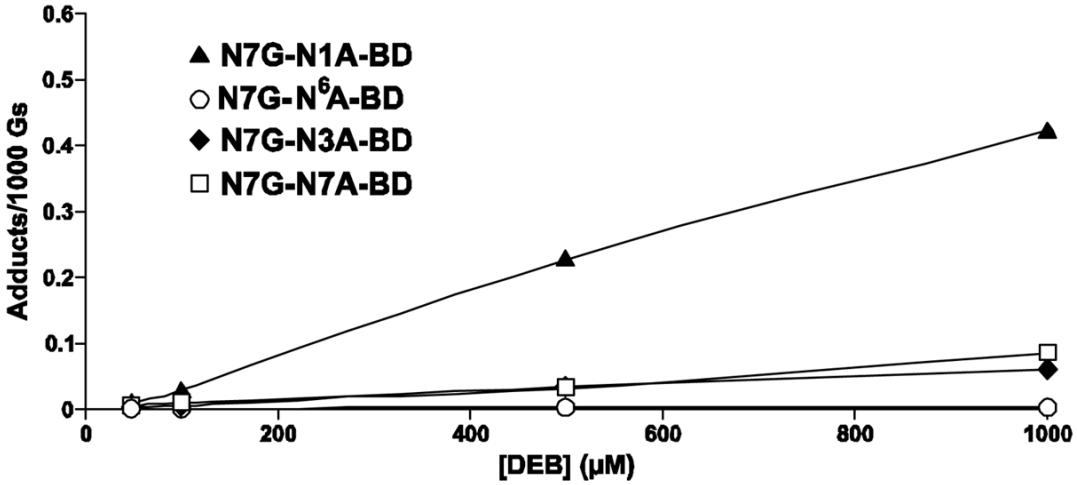

Figure 3.
Formation of regioisomeric Gua-Ade-BD cross-links in calf thymus DNA exposed to racemic DEB (0–1000 μM).

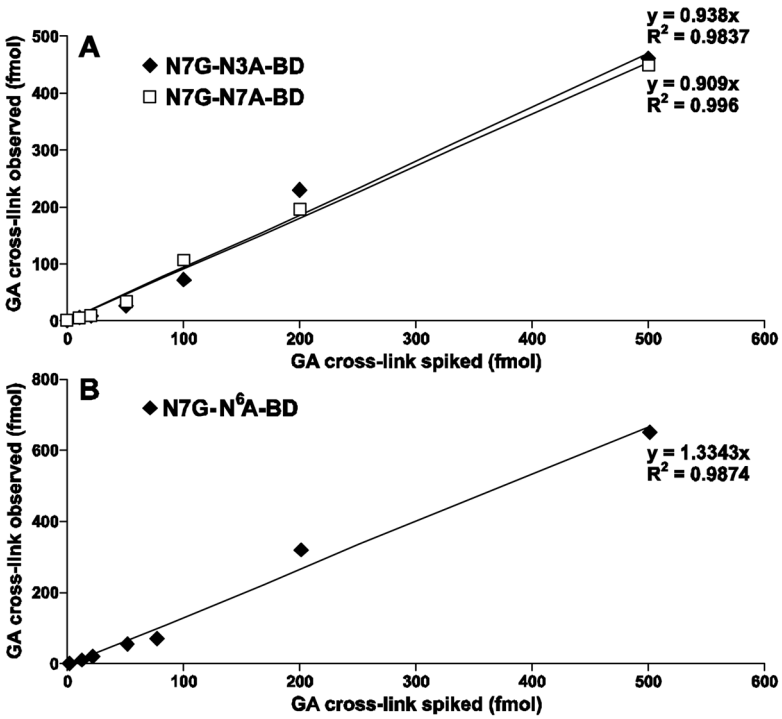

Figure 4.

Correlation between expected and measured levels of N7G-N3A-BD, N7G-N7A-BD (A) and N7G-N^{6}A-BD (B) in mouse liver DNA (0.1 mg) spiked with known amounts of N7G-Ade-BD adducts (0–500 fmol).

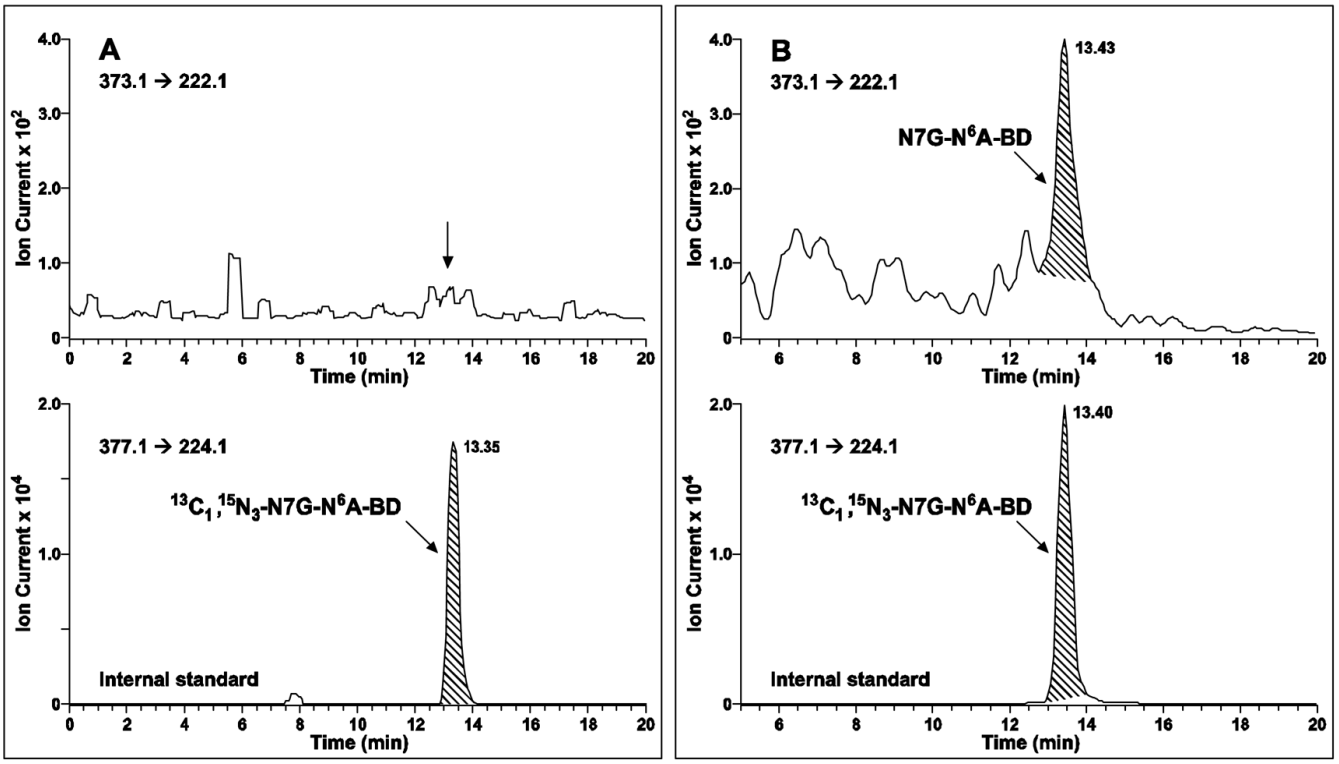

Figure 5.

Representative HPLC-ESI$^+$-MS/MS traces for analyses of N7G-N^{6}A-BD in acid hydrolysates of liver DNA extracted from control (A) and BD-exposed female B6C3F1mice (625 ppm for 10 days) (B).

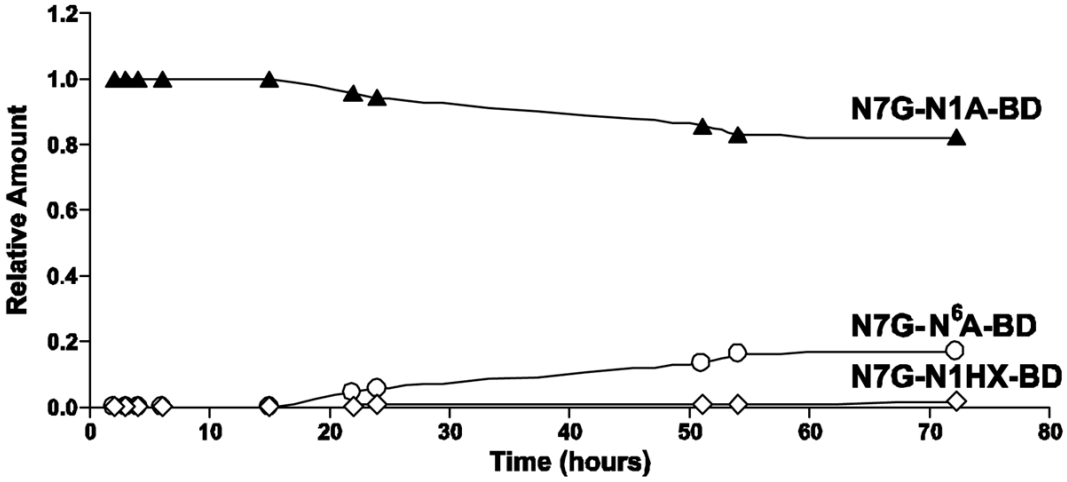

Figure 6.
Kinetics of Dimroth rearrangement and hydrolytic deamination of N7G-N1A-BD at physiological conditions (37 °C and pH 7.4).

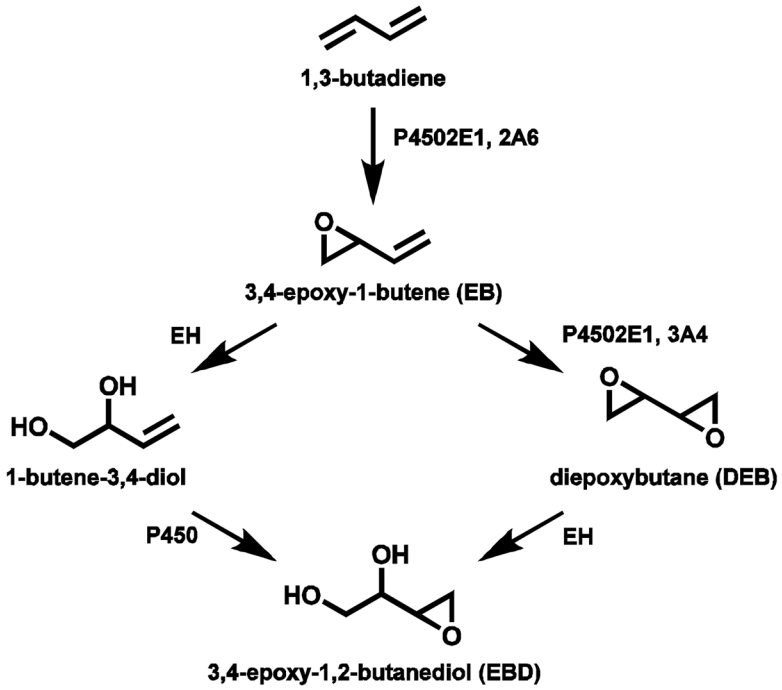

Scheme 1.
Metabolism of 1,3-butadiene to DNA-reactive epoxides.

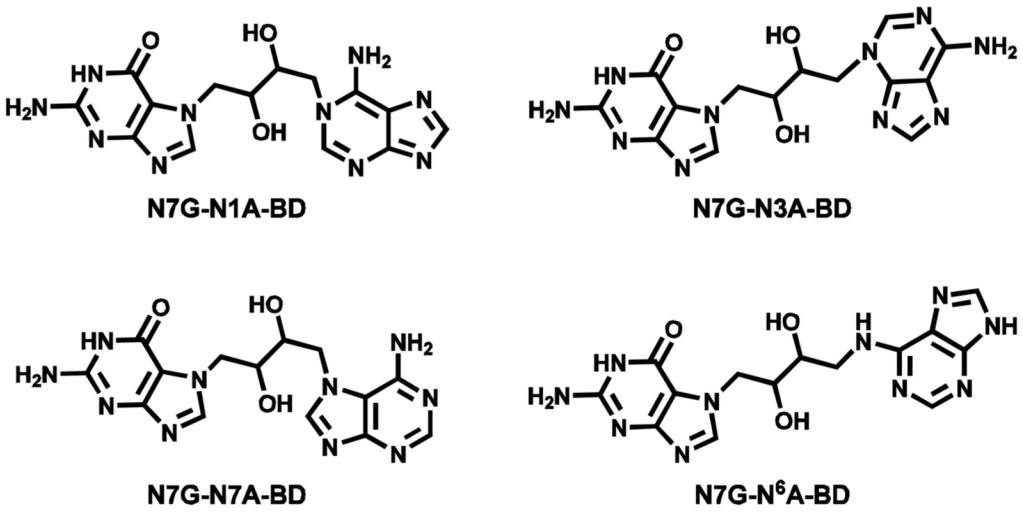

Scheme 2.

Chemical structures of regioisomeric guanine-adenine (G-A) cross-links: 1-(guan-7-yl)-4-(aden-1-yl)-2,3-butanediol (N7G-N1A-BD), 1-(guan-7-yl)-4-(aden-3-yl)-2,3,-butanediol (N7G-N3A-BD), 1-(guan-7-yl)-4-(aden-7-yl)-2,3-butanediol (N7G-N7A-BD), and 1-(guan-7-yl)-4-(aden-6-yl)-2,3-butanediol (N7G-N^6A-BD).

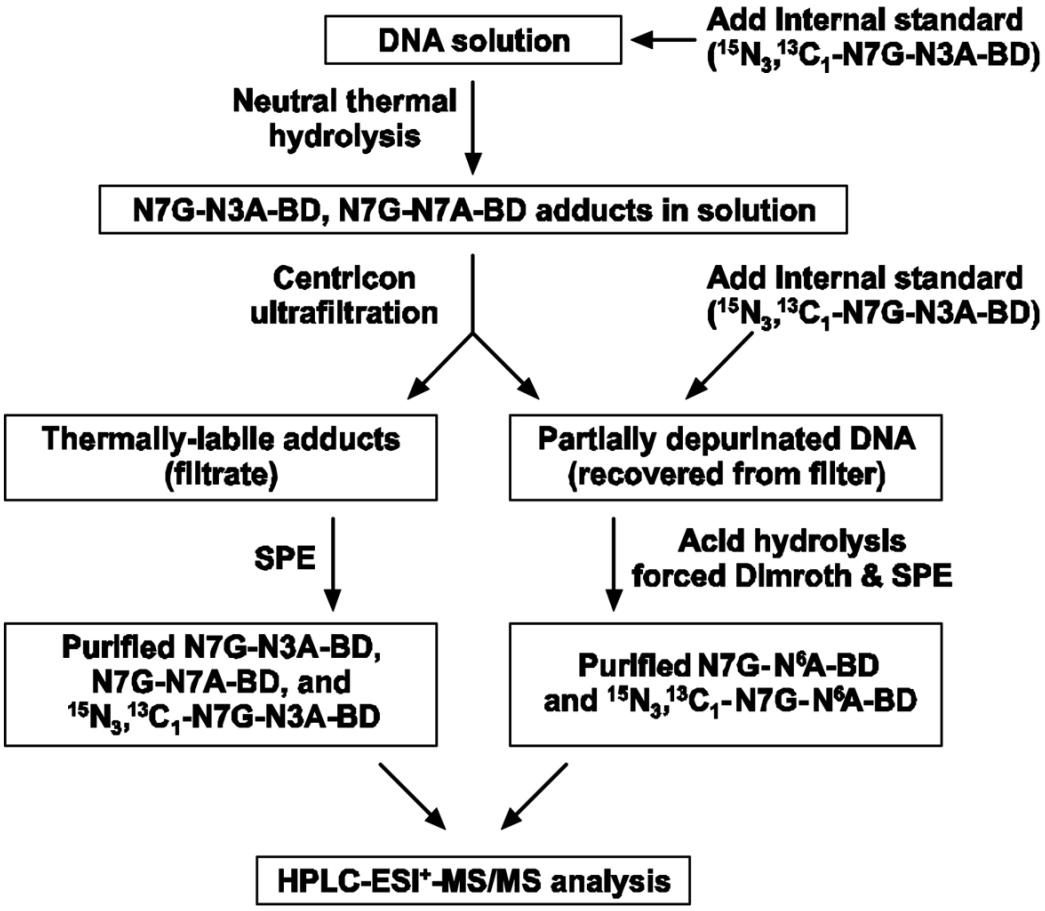

Scheme 3.
Experimental scheme for quantitative HPLC-ESI$^+$-MS/MS analyses of G-A DEB cross-links.

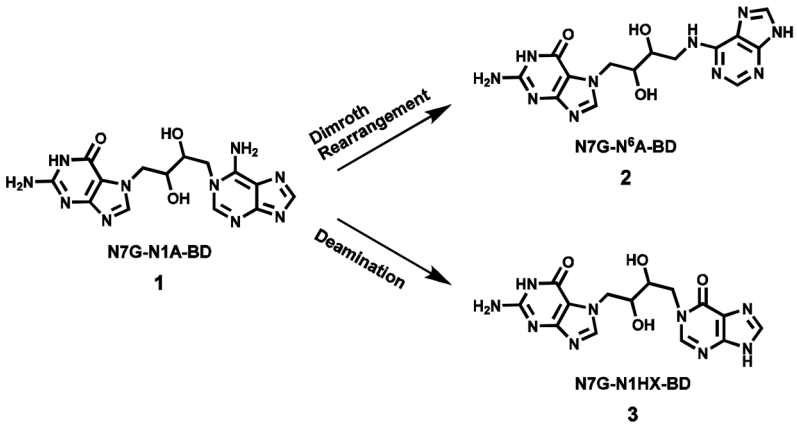

Scheme 4.

Dimroth rearrangement and hydrolytic deamination of 1-(guan-7-yl)-4-(aden-1-yl)-2,3-butanediol (N7G-N1A-BD) at physiological conditions.

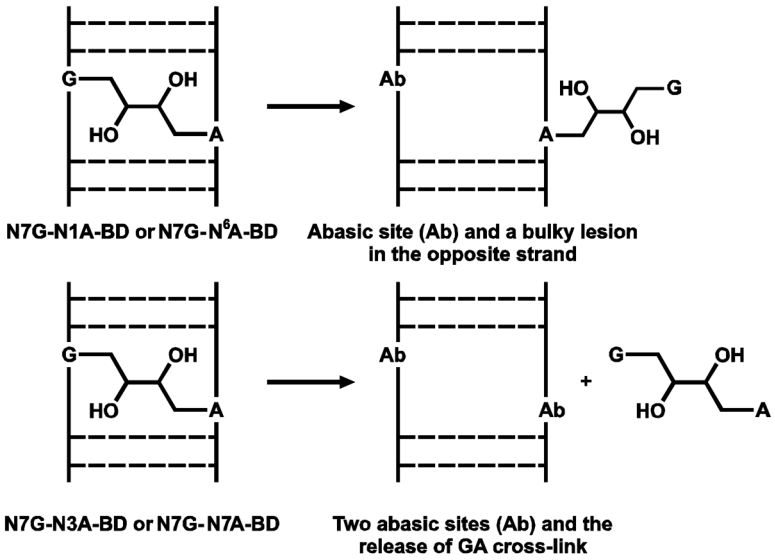

Scheme 5.
Spontaneous hydrolysis of regioisomeric guanine-adenine DEB conjugates.

Table 1

Validation results for HPLC-ESI$^+$-MS/MS analysis of N7G-N3A-BD, N7G-N7A-BD, and N7G-N^{6}A-BD (10 fmol) spiked into mouse liver DNA (0.1 mg) using N3A and N1A forms of [$^{15}N_3$, $^{13}C_1$] internal standards.

		N7G-N3A-BD	N7G-N7A-BD	N7G-N^{6}A-BD
Day 1	mean	11.3	10.3	7.89
	RSD (%)	12.9	25.9	11.4
	accuracy (%)	113	103	78.9
	n	5	5	5
Day 2	mean	11.1	11.9	7.66
	RSD (%)	12.9	15.5	2.98
	accuracy (%)	111	119	76.6
	n	5	5	5
Day 3	mean	8.1	8.88	8.56
	RSD (%)	9.3	12	16.5
	accuracy (%)	81	88.8	85.6
	n	3	3	3
Interday	mean	10.5	10.2	7.94
	RSD (%)	17.4	25.4	10.6
	accuracy (%)	105	102	79.4
	n	13	13	13

Table 2

Quantitative analysis of N7G-Ade-BD in liver DNA (0.1 mg) of control and BD-exposed (625 ppm for 10 days) female B6C3F1 mice.

	N7G-N3A-BD per10^8 nts	N7G-N7A-BD per10^8 nts	N7G-N1A-BD + N7G-N^6A-BD per 10^8 Nts
Control mouse liver DNA (n = 4)	< 0.64	< 0.64	< 0.64
BD-exposed (625 ppm) mouse liver DNA (n = 5)	< 0.64	< 0.64	3.1 ± 0.6